

<https://doi.org/10.1038/s42004-026-01948-1>

# Electrochemical Ferrier rearrangement of glycals in flow



Pallav Suman<sup>1</sup>, Mihhail Fokin<sup>1</sup>, Kaarel Erik Hunt<sup>1</sup>, Tõnis Kanger<sup>1</sup>, Daniele Mazzarella<sup>2</sup>✉ & Maksim Ošek<sup>1</sup>✉

The Ferrier rearrangement is a cornerstone transformation in carbohydrate chemistry, typically requiring strongly acidic or oxidative conditions. Here we report a continuous-flow electrochemical Ferrier rearrangement operating in an undivided microreactor equipped with inexpensive graphite electrodes mitigating batch process limitations, such as insufficient mass transfer and charge utilization. The process proceeds efficiently with minimal supporting electrolyte and charge input, converting a wide range of acyloxy- and alkoxyglycals with diverse oxygen-, sulfur-, nitrogen-, and carbon-based nucleophiles to 2,3-unsaturated glycosides in up to 94% yield and excellent diastereoselectivity. The short interelectrode distance enables completion under 20 seconds residence time, affording gram-scale productivity ( $10 \text{ mmol} \cdot \text{h}^{-1}$ ) and high faradaic efficiency. Mechanistic and electrochemical data support a radical-chain pathway initiated by anodic oxidation of glycal. This operationally simple and scalable protocol advances electrochemical glycosylation toward sustainable, industry-relevant synthesis.

The Ferrier rearrangement (FR) enables the conversion of glycals **1** (Fig. 1a) into synthetically versatile 2,3-unsaturated glycosides **3'**, important building blocks in numerous bioactive molecules such as spliceostatin<sup>2</sup>, paclitaxel<sup>3</sup>, and several antibiotics like capuramycin<sup>4,5</sup> (Fig. 1b). Classical FR protocols rely on strong Brønsted or Lewis acids (e.g.  $\text{CF}_3\text{CO}_2\text{H}$ <sup>6</sup>,  $\text{TfOH}$ <sup>7</sup>,  $\text{BF}_3 \cdot \text{Et}_2\text{O}$ <sup>8</sup>,  $\text{SnCl}_4$ <sup>9</sup>,  $\text{I}_2$ <sup>10</sup>) that promote the formation of allylic oxocarbenium ion **A** from a suitably activated glycal derivative **1**, decorated with a good leaving group at the C-3 position. Alternatively, single electron oxidation can generate radical cation **B**, which subsequently expels a radical fragment to form intermediate **A**. Such oxidative variants employ (sub)stoichiometric amounts of oxidants, including  $(\text{NH}_4)_2[\text{Ce}(\text{NO}_3)_6]$ <sup>11,12</sup> or  $\text{K}_5\text{CoW}_{12}\text{O}_4$ <sup>13</sup>. While effective, these protocols often rely on corrosive acids and hazardous oxidizing reagents, both notorious for their impact on environmental sustainability, and responsible for a considerable amount of waste generation. Some mild and eco-friendly FR methodologies employing microwave irradiation<sup>14</sup> and deep eutectic solvents<sup>15</sup> have also been reported. However, their broader applicability is still constrained by scale-up challenges and a relatively limited substrate scope.

Organic electrochemistry has recently re-emerged as a powerful platform for redox transformations<sup>16</sup>, replacing chemical oxidants and reductants with electric current as an inexpensive, renewable, and inherently safe reagent<sup>17,18</sup>. Recently, we have demonstrated, the feasibility of performing the FR under undivided electrochemical conditions using inexpensive

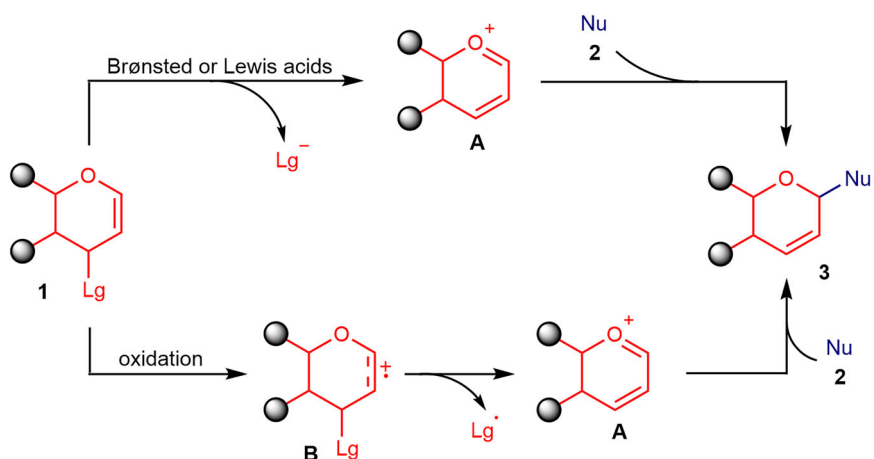
electrodes and mild reaction conditions<sup>19</sup>. This approach exhibited broad substrate compatibility, accommodating a wide range of glycal derivatives **1** and nucleophiles **2**. Nonetheless, this approach suffered from long reaction times, large amounts of supporting electrolyte, and a high excess of charge input, common drawbacks of batch electrolysis.

Continuous-flow electrochemistry, by contrast, offers superior mass and heat transfer due to short diffusion paths<sup>20</sup>. Moreover, a larger surface-to-volume ratio significantly reduces the reaction time, while the short interelectrode gap in flow reactors lowers Ohmic voltage drop, thereby minimizing the need for supporting electrolytes<sup>21</sup>. Flow technology has thus become integral to modern organic electrochemistry, offering enhanced efficiency, sustainability and scalability, making it highly attractive for industrial implementation<sup>22</sup>. The Nagaki group<sup>23</sup> reported the development of a novel flow electrochemical reactor<sup>20</sup>, capable of producing cationic intermediates for FR within very short residence times by adopting the “cation pool” strategy (Fig. 2a)<sup>24</sup>. In this approach, they afforded a stoichiometric amount of the oxonium ion **A** by flash electrolysis and subsequently intercepted it by nucleophiles **2** before its decomposition. Another flow electrochemical variant of FR was later reported by Sato and Suga featuring one synthetic example **3a** with moderate yield (Fig. 2b)<sup>25</sup>. However, these protocols are constrained by the need for highly sophisticated divided-cell flow setups, costly platinum electrodes,<sup>26</sup> cryogenic conditions, and a limited substrate scope, overall

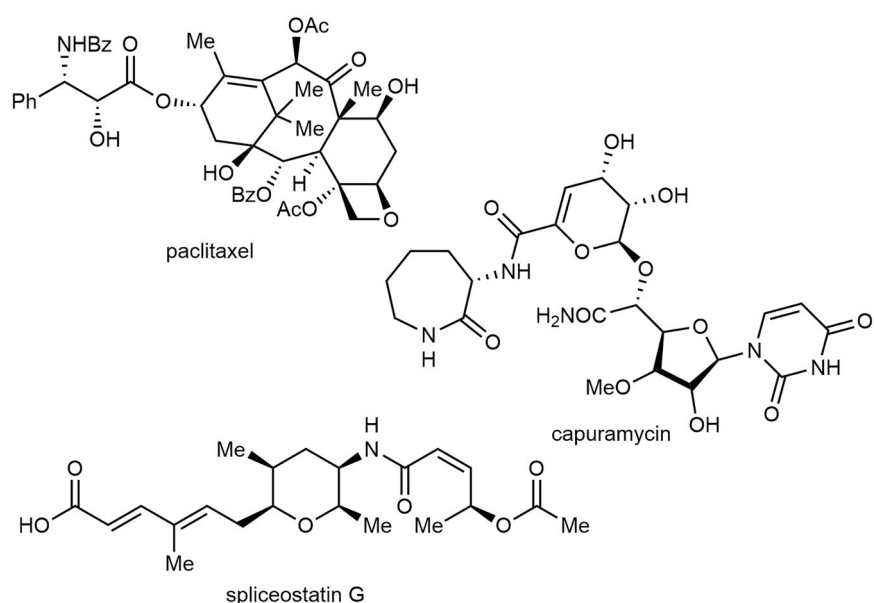
<sup>1</sup>Department of Chemistry and Biotechnology, Tallinn University of Technology, Akadeemia tee 15, 12618 Tallinn, Estonia. <sup>2</sup>Department of Chemical Sciences and Technologies, University of Rome Tor Vergata, Via della Ricerca Scientifica 1, 00133 Rome, Italy. ✉e-mail: [daniele.mazzarella@uniroma2.it](mailto:daniele.mazzarella@uniroma2.it); [maksim.oseka@taltech.ee](mailto:maksim.oseka@taltech.ee)

**Fig. 1 | Ferrier rearrangement and its application.**  
**a** Classical and oxidative Ferrier rearrangement.  
**b** Bioactive compounds obtained *via* Ferrier rearrangement as a key step.

**a) Acidic and oxidative Ferrier rearrangement**



**b) Bioactive molecules synthesized using Ferrier rearrangement**



compromising their potential to be employed in an industrial application.

Building on our experience in handling sensitive intermediates and products under electrochemical flow conditions<sup>27–29</sup>, we now report an operationally simple, efficient, and scalable FR in an undivided flow setup. The process requires inexpensive electrodes and only minimal amount of supporting electrolyte and electrical charge input (Fig. 2c). Overall, this approach advances FR toward more sustainable and industry-relevant electrochemical synthesis.

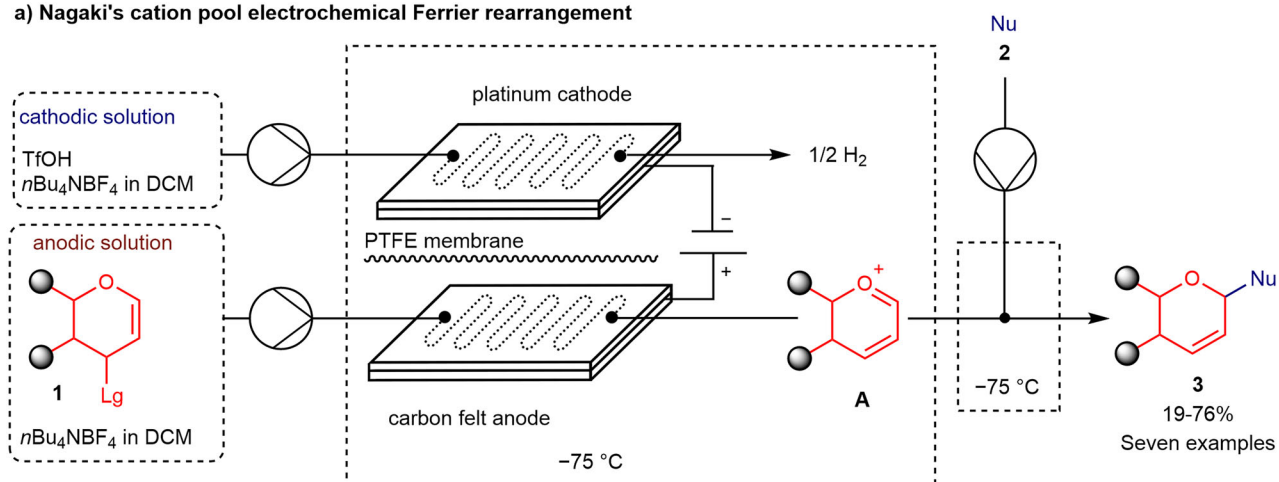
## Results and discussion

Our investigation commenced with the introduction of commercially available tri-*O*-acetyl-D-glucal **1a** and benzyl alcohol **2b** into an undivided electrochemical microflow reactor (300  $\mu$ L internal volume) equipped with an impervious-graphite anode and regular graphite cathode (Table 1) (see Supplementary Information, Figure S1)<sup>30</sup>. Based on our previously reported batch electrochemical FR<sup>19</sup>, where acetonitrile was identified as the optimal solvent, we rapidly optimized the reaction to the undivided continuous-flow setup, affording the desired product **3b** in 94% yield, in only 2 min of residence time ( $t_R$ ) under galvanostatic conditions in acetonitrile (entry 1). The excess of benzyl alcohol was required to obtain high yield of the desired

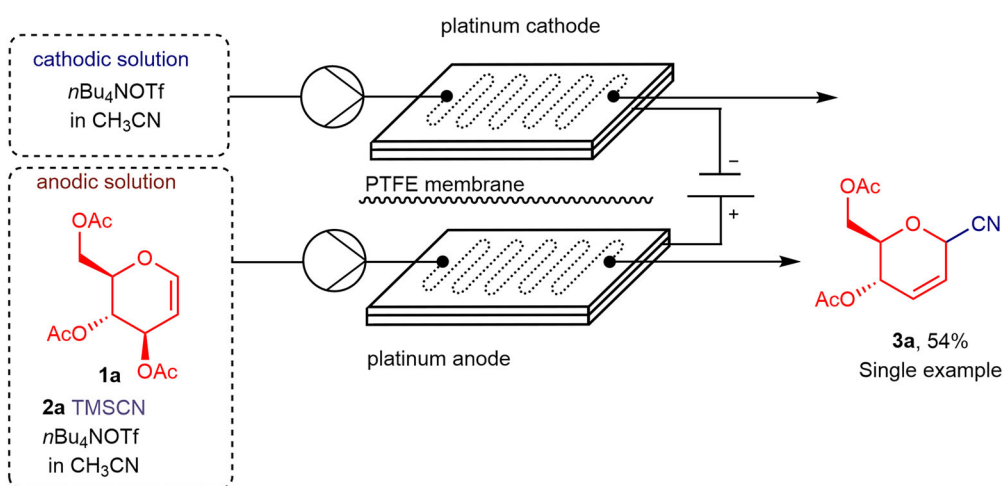
product, while lowering the amount of nucleophile resulted in the formation of side products. Notably, the 250  $\mu$ m inter-electrode gap enabled a drastic reduction of electrolyte loading (0.1 equiv.) without compromising the yield<sup>22</sup>. Decreasing the substrate concentration (entry 2) or applied charge (entry 3) led to slightly lower yields, whereas increasing the charge (entry 4) led to undesired oxidation of benzyl alcohol **2b** to benzaldehyde. The reaction remained highly efficient even at shorter  $t_R$  (entries 5 and 6), underscoring the potential for high productivity under continuous-flow conditions, though a 2-minute residence time was selected for practicality. Variations in electrolytes from *n*Bu<sub>4</sub>NClO<sub>4</sub> to *n*Bu<sub>4</sub>NBF<sub>4</sub> (entry 7) or *n*Bu<sub>4</sub>NPF<sub>6</sub> (entry 8) proved to be detrimental for the yield, while the use of inert or anhydrous conditions (entries 9 and 10) had little effect on the overall process. Alternative electrode combinations (entries 11 and 12) led to reduced yields. As expected, the reaction was confirmed to be electrochemical in nature, as no conversion occurred in the absence of applied current (entry 13).

Having established the optimal reaction conditions, we next turned our attention to evaluating the generality of this process (Fig. 3). We began by exploring the scope of various glycol derivatives in combination with benzyl alcohol **2b**. Consistent with the batch reaction<sup>19</sup>, our electrochemical flow protocol was not limited to glycols bearing an acetyl leaving group at the C-3

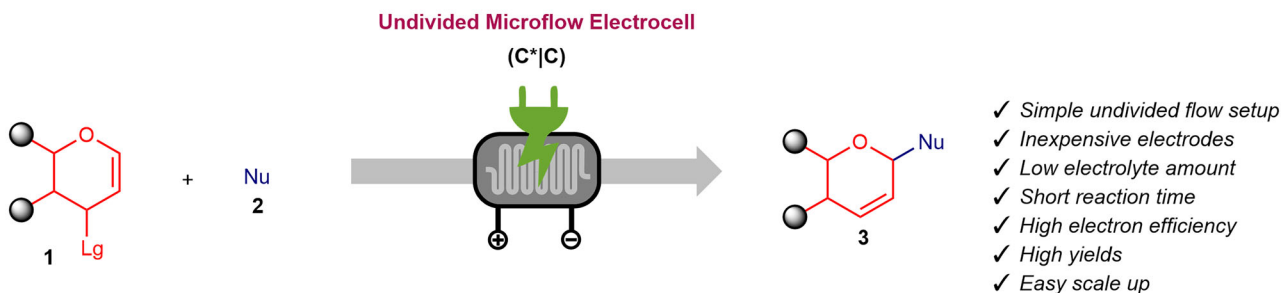
## a) Nagaki's cation pool electrochemical Ferrier rearrangement



## b) Sato and Suga's carbon electrochemical Ferrier rearrangement



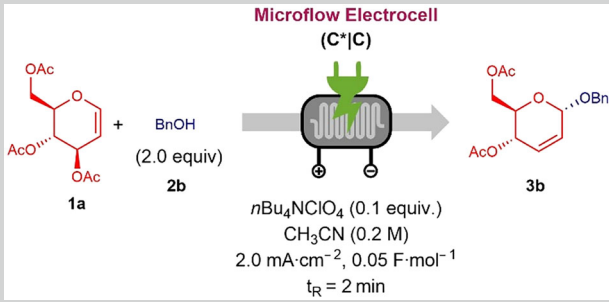
## c) This work: electrochemical Ferrier rearrangement of glycols in flow



**Fig. 2 | Electrochemical Ferrier rearrangements in flow.** **a** Nagaki's protocol in a divided cell under cryogenic conditions. **b** Sato and Suga's protocol in a divided cell with one example. **c** This work.

position (compound **3b**) but was also compatible with the benzyl-protected derivative, affording the desired product **3c** in high yield (see Supplementary Information, Figure S2 for starting materials). Furthermore, extending the methodology to D-galactose-derived glycal provided the corresponding 2,3-unsaturated glycoside **3d** in good yield, confirming the applicability of this microflow electrochemical approach. We then investigated the scope of nucleophiles. Various alcohols were tested: ethanol, *n*-hexanol and L-menthol afforded **3e-3g** in excellent yields. When tetra-*O*-acetyl-D-glucose<sup>31</sup> was employed as the nucleophile, the corresponding disaccharide **3h** was obtained. Next, we explored carbon-based nucleophiles to enable C-C bond formation. Electrochemical glycosylation with trimethylsilyl

cyanide yielded **3a** in significantly higher yield compared to the previously reported method by Sato and Suga<sup>25</sup>. When allyltrimethylsilane and silyl enol ether were used, the desired alkylated products **3i** and **3j** were obtained in high yields. Finally, using 1-phenyl-2-trimethylsilylacetylene as the reaction partner enabled the construction of a C(sp<sup>3</sup>)-C(sp) bond (compound **3k**). Furthermore, the oxidation of glycal **1a** in the presence of Et<sub>3</sub>SiH furnished the product **3l** in excellent yield. Notably, reaction with trimethylsilyl azide as the nucleophile was also successful, providing glycosyl azide **3m** exclusively in 94% yield, assessed by <sup>1</sup>H NMR spectroscopy of the crude mixture. However, during workup procedure, glycosyl azide **3m** partially underwent a [3,3]-sigmatropic rearrangement and was isolated as

**Table 1 | Optimization of reaction conditions**


Entry	Variations from the standard conditions	Yield (%) <sup>b</sup>
1 <sup>a</sup>	none	94 (86) <sup>c</sup>
2	0.1 M, 2.5 mA·cm <sup>-2</sup> , 0.1 F·mol <sup>-1</sup>	85
3	1.0 mA·cm <sup>-2</sup> , 0.025 F·mol <sup>-1</sup>	72
4	4.0 mA·cm <sup>-2</sup> , 0.1 F·mol <sup>-1</sup>	93
5	t <sub>R</sub> = 1 min, 4.0 mA·cm <sup>-2</sup>	94
6	t <sub>R</sub> = 18 s, 13.3 mA·cm <sup>-2</sup>	91
7	<i>n</i> Bu <sub>4</sub> NBF <sub>4</sub> as electrolyte	26
8	<i>n</i> Bu <sub>4</sub> NPF <sub>6</sub> as electrolyte	89
9	under argon	94
10	dry CH <sub>3</sub> CN	92
11	graphite anode	traces
12	stainless steel cathode	20
13	no electricity	0

<sup>a</sup> Reaction conditions: tri-*O*-acetyl-D-glucal **1a** (1.0 equiv.), benzyl alcohol **2b** (2.0 equiv.), *n*Bu<sub>4</sub>NClO<sub>4</sub> (0.1 equiv.), CH<sub>3</sub>CN (0.2 M), impervious graphite anode/graphite cathode, 2.0 mA·cm<sup>-2</sup>, 0.05 F·mol<sup>-1</sup>, room temperature, 0.15 mL·min<sup>-1</sup> flow rate, 2 min residence time. <sup>b</sup> Yields were determined by <sup>1</sup>H NMR analysis of the crude mixture, using diglyme as an internal standard. <sup>c</sup> Isolated yield.

C-1/C-3 isomeric mixture in 89% yield<sup>32-34</sup>. Additionally, employing *p*-toluenesulfonamide as the nucleophile afforded the corresponding 2,3-unsaturated glycoside **3n** in very good yield. Importantly, aliphatic sulfur nucleophiles were also found to be compatible with the reaction conditions (products **3o** and **3p**). However, the yields were significantly lower compared to those obtained *via* the previously reported batch protocol.<sup>19</sup> This indicates that, although aliphatic sulfur nucleophiles can participate in the transformation, their diminished reactivity sets the limitation for our methodology. On the contrary, when thiophenol was tested as nucleophile, the corresponding product **3q** was isolated in excellent yield, despite the low oxidation potential of thiophenol. Some unprotected glycals and nucleophiles were not compatible with the reaction conditions giving a range of side products or stayed unreactive (see Supplementary Information, section 5). Lastly, the products were obtained in diastereomeric ratios in line with the previous electrochemical contributions<sup>19,23,25</sup>, while the yields are considerably higher, underscoring the efficiency of this electrochemical flow transformation.

We further evaluated the scalability of this methodology by performing a multi-gram reaction of **1a** (10 mmol) and **2b** (see Supplementary Information, section 4). In flow synthesis, productivity is strongly influenced by the flow rates; thus, a faster flow rate without compromising yield is crucial. For this scale-up experiment, a flow rate of 1 mL·min<sup>-1</sup> (residence time 18 s) was employed. The reaction proceeded efficiently under these conditions, delivering **3b** with a productivity of 10.2 mmol per hour (3.27 g·h<sup>-1</sup>) and achieving a space-time yield of 10.9 Kg·L<sup>-1</sup>·h<sup>-1</sup>. Conversion of starting material **1a** and yield of product **3b** remained consistent throughout the entire 50-minute collection period. Furthermore, during reaction optimization no residence time limit was reached at which the yield began to decrease. These findings suggest that productivity could be further enhanced at even higher flow rates.

To demonstrate the sustainability of the developed protocol, its green chemistry metrics were compared with other electrochemical FR methods using the standardized CHEM21 toolkit<sup>35</sup> (Table 2). In particular, the divided-cell approach reported by Nagaki<sup>23</sup> and our previously reported batch method<sup>19</sup> were selected for comparison, both applied to the synthesis of compound **3i** from glucal **1a** and allyltrimethylsilane. Our highly efficient chain process not only avoids the use of highly hazardous compounds and cryogenic conditions but also affords product **3i** in higher yield. Moreover, the process mass intensity (PMI) was significantly improved due to the reduced electrolyte loading and the higher reaction mixture concentration.

After establishing the sustainability and synthetic utility of this undivided microfluidic electrochemical FR, we investigated its reaction mechanism. The exceptionally high faradaic efficiency observed under flow conditions, together with supporting evidence from the previous literature reports<sup>25,36</sup> and cyclic voltametric data<sup>19</sup>, suggests a radical chain mechanism (Fig. 4). The process is initiated by the anodic oxidation of tri-*O*-acetyl-D-glucal **1a**, generating radical cation **B**. Loss of the acetoxy radical from **B** affords oxonium ion intermediate **A**, which is subsequently intercepted by a nucleophile, here benzyl alcohol **2b**, to yield 2,3-unsaturated glycosyl derivative **3b** upon deprotonation. The acetoxy radical is then reduced to the acetate by oxidizing another molecule of glucal **1a**, regenerating radical cation **B** and thereby propagating the chain process. The chain is terminated through reduction of the acetoxy radical at the cathode. The choice of anode material is critical: only impervious graphite efficiently promoted the formation of the desired product, whereas other electrodes gave no conversion. Although further studies are needed to confirm this, the high performance of impervious graphite is likely due to its resistance to adsorption or surface grafting of chemical species, which can inhibit electron transfer from the substrate to the electrode<sup>37</sup>. Reversible surface interactions further facilitate efficient

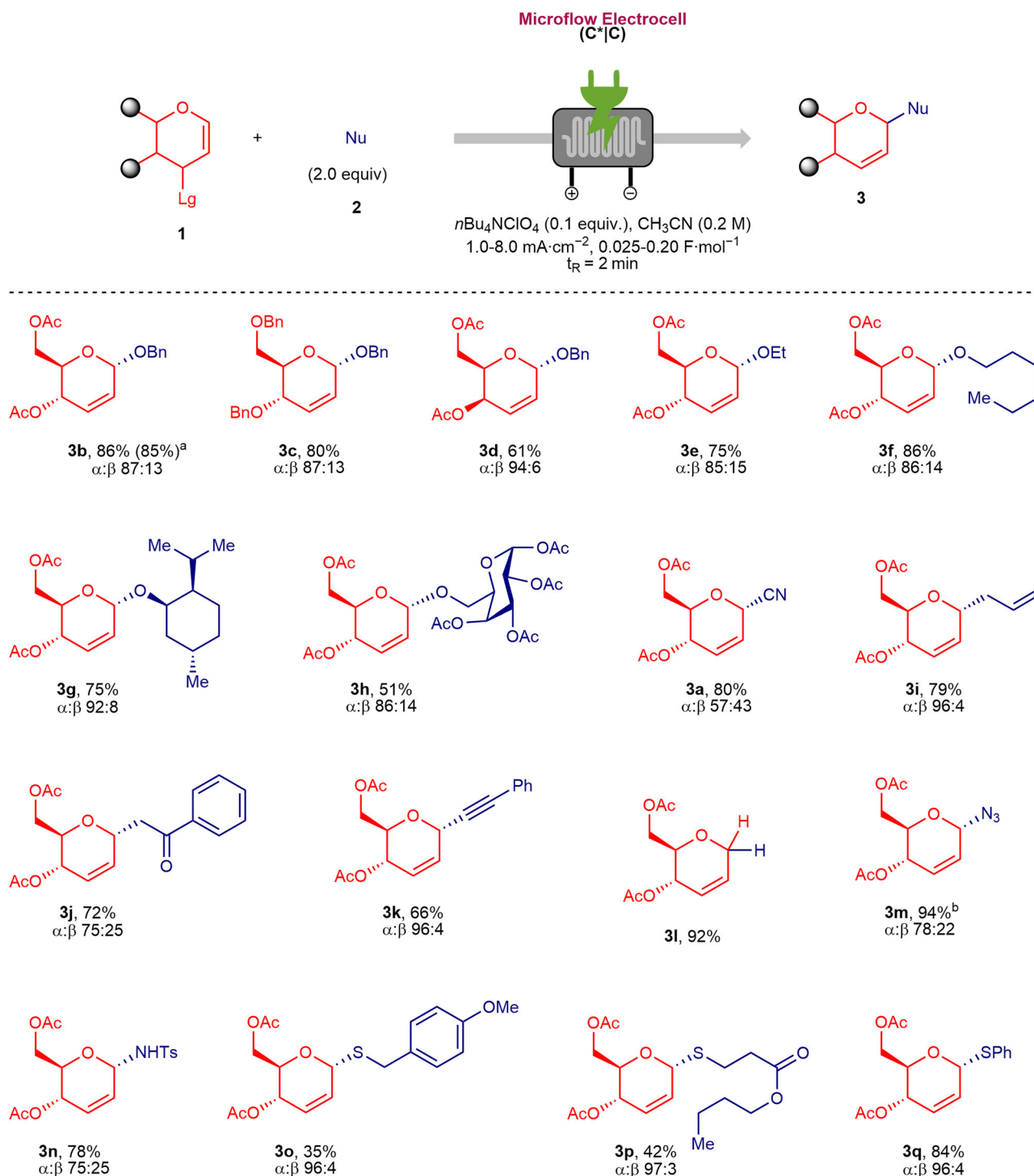


**Fig. 3 | Substrate scope.** Reaction conditions: glycol 1 (1.0 equiv.), nucleophile 2 (2.0 equiv.),  $n\text{Bu}_4\text{NClO}_4$  (0.1 equiv.),  $\text{CH}_3\text{CN}$  (0.2 M), impervious graphite anode/graphite cathode, 1.0-8.0  $\text{mA}\cdot\text{cm}^{-2}$ , 0.025-0.20  $\text{F}\cdot\text{mol}^{-1}$ , room temperature, 0.15  $\text{mL}\cdot\text{min}^{-1}$  flow rate, 2 min residence time, collected for 33.3 min. Yields

correspond to isolated products. Diastereomeric ratios were determined by  $^1\text{H}$  NMR analysis of isolated products. <sup>a</sup> Scale up experiment: 1.0  $\text{mL}\cdot\text{min}^{-1}$  flow rate, 18 s residence time, collected for 50 min. <sup>b</sup> Yield was determined by  $^1\text{H}$  NMR analysis of the crude mixture, using diglyme as an internal standard.

charge transfer, while enhanced mass transfer under flow conditions accelerates the overall reaction. We attribute the optimal efficiency of our electrochemical protocol to this combination of reduced surface fouling and improved electron and mass transfer.

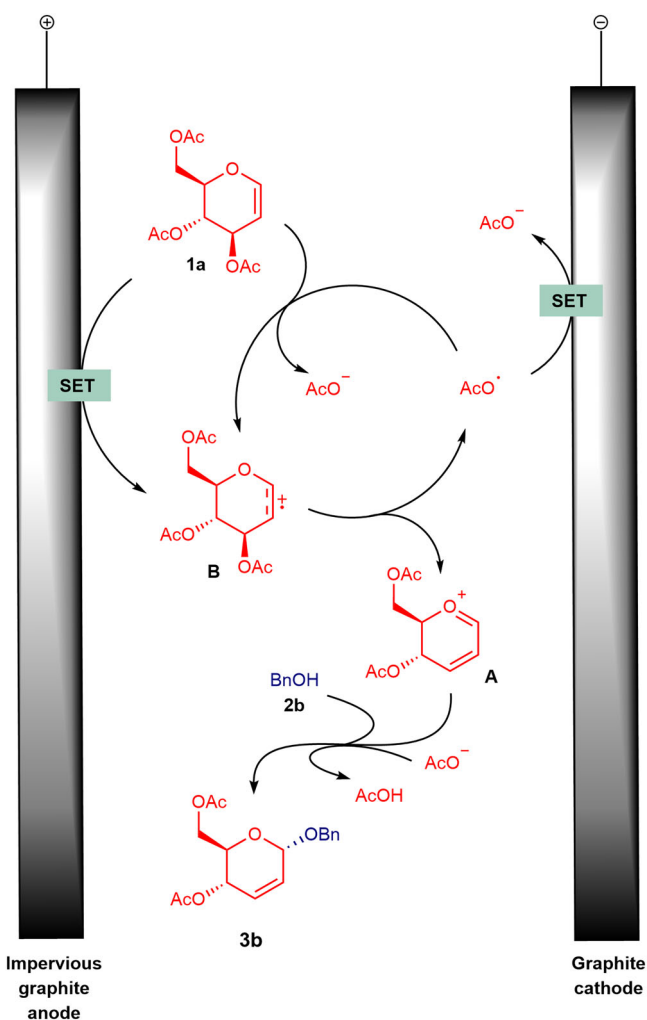
## Conclusion

In summary, we have developed a continuous-flow electrochemical Ferrier rearrangement in an undivided microreactor using inexpensive

electrodes. The process proceeds under mild conditions with minimal amount of supporting electrolyte and charge, delivering a broad range of 2,3-unsaturated glycosyl derivatives in high yields and with excellent faradaic efficiency. This advance transforms the Ferrier rearrangement into a sustainable, industrially relevant electrochemical process and establishes a foundation for scalable electrochemical glycosylations.

**Table 2 | Comparison of the green chemistry metrics**

	Divided cell <sup>23</sup>	Batch <sup>19</sup>	This work
Reaction type	single electron process (1.25 F·mol <sup>-1</sup> )	single electron process (2.3 F·mol <sup>-1</sup> )	chain process (0.05 F·mol <sup>-1</sup> )
Temperature	-75 °C	rt	rt
Solvent	CH <sub>2</sub> Cl <sub>2</sub>	CH <sub>3</sub> CN	CH <sub>3</sub> CN
Health concerns	H290, H302, H314, H315, H319, H335, H336, H351		
Yield of <b>3i</b> (%)	74	68	79
PMI (without workup)	979	98	22

**Fig. 4 | Proposed mechanism.** SET – single electron transfer oxidation on anode and reduction on cathode.

## Methods

### General procedure for electrochemical Ferrier rearrangement in flow

A solution of glycal **1** (2.0 mmol, 1.0 equiv.), nucleophile **2** (4.0 mmol, 2.0 equiv.) and *n*Bu<sub>4</sub>NClO<sub>4</sub> (0.2 mmol, 0.1 equiv.) in CH<sub>3</sub>CN (0.2 M) was

loaded into a 10 mL syringe and pumped through an undivided micro-reactor (300 μL of internal volume) at 0.15 mL·min<sup>-1</sup> (2 min residence time) under constant current at room temperature. After reaching steady state after 10 minutes, the product solution was collected for 33 min and 20 seconds, corresponding to 1.0 mmol of product. The resulting reaction mixture was then concentrated under reduced pressure, and the crude was purified by flash column chromatography on silica gel to afford corresponding product **3**. The structures of compounds **3a–q** were unambiguously confirmed by NMR spectroscopy (see Supplementary Information, Figures S4–S37).

### Data availability

The data supporting the findings of this study are included in the paper or the Supplementary Information and are also available upon request from the corresponding author. The Supplementary Information contains full details of the experimental procedure, electrochemical flow setup description, characterization of compounds, supplementary references, copies of <sup>1</sup>H NMR and <sup>13</sup>C NMR spectra.

Received: 27 November 2025; Accepted: 9 February 2026;

Published online: 25 February 2026

## References

1. Ferrier, R. J., Overend, W. G. & Ryan, A. E. The reaction between 3,4,6-tri-*O*-acetyl-D-glucal and *p*-nitrophenol. *J. Chem. Soc.* 3667–3670 (1962).
2. Ghosh, A. K., Reddy, G. C., MacRae, A. J. & Jurica, M. S. Enantioselective Synthesis of Spliceostatin G and Evaluation of Bioactivity of Spliceostatin G and Its Methyl Ester. *Org. Lett.* **20**, 96–99 (2018).
3. Fukaya, K. et al. Synthesis of Paclitaxel. 2. Construction of the ABCD Ring and Formal Synthesis. *Org. Lett.* **17**, 2574–2577 (2015).
4. Pigman, W. *The Carbohydrates: Chemistry And Biochemistry Physiology*. (Academic Press, 2012).
5. Kusaka, S., Yamamoto, K., Shinohara, M., Minato, Y. & Ichikawa, S. Synthesis of capuramycin and its analogues via a Ferrier-type I reaction and their biological evaluation. *Bioorg. Medicinal Chem.* **73**, 117011 (2022).
6. Fuertes, M., García-Muñoz, G., Lora-Tamayo, M., Madroñero, R. & Stud, M. Benzotriazole glycosides from glycals. *Tetrahedron Lett.* **9**, 4089–4092 (1968).
7. Bhuma, N. et al. Insight into the Ferrier Rearrangement by Combining Flash Chemistry and Superacids. *Angew. Chem. Int Ed.* **60**, 2036–2041 (2021).
8. Ferrier, R. J. & Prasad, N. Unsaturated carbohydrates. Part IX. Synthesis of 2,3-dideoxy- $\alpha$ -D-erythro-hex-2-enopyranosides from tri-*O*-acetyl-D-glucal. *J. Chem. Soc. C* 570–575 (1969).
9. Gryniewicz, G., Priebe, W. & Zamojski, A. Synthesis of alkyl 4,6-di-*O*-acetyl-2,3-dideoxy- $\alpha$ -D-threo-hex-2-enopyranosides from 3,4,6-tri-*O*-acetyl-1,5-anhydro-2-deoxy-D-lyxo-hex-1-enitol (3,4,6-tri-*O*-acetyl-D-galactal). *Carbohydr. Res.* **68**, 33–41 (1979).
10. Koreeda, M., Houston, T. A., Shull, B. K., Klemke, E. & Tuinman, R. J. Iodine-catalyzed Ferrier Reaction 1. A Mild and Highly Versatile Glycosylation of Hydroxyl and Phenolic Groups 1. *Synlett* **1995**, 90–92 (1995).
11. Devari, S., Kumar, M., Deshidi, R., Rizvi, M. & Shah, B. A. A general metal-free approach for the stereoselective synthesis of C-glycals from unactivated alkynes. *Beilstein J. Org. Chem.* **10**, 2649–2653 (2014).
12. Yadav, J. S., Subba Reddy, B. V. & Pandey, S. K. Ceric(IV) ammonium nitrate-catalyzed glycosidation of glycals: a facile synthesis of 2,3-unsaturated glycosides. *N. J. Chem.* **25**, 538–540 (2001).
13. Rafiee, E., Tangestaninejad, S., Habibi, M. H. & Mirkhani, V. A mild, efficient and  $\alpha$ -selective glycosidation by using potassium

- dodecatungstocobaltate trihydrate as catalyst. *Bioorg. Medicinal Chem. Lett.* **14**, 3611–3614 (2004).
14. Shanmugasundaram, B., Bose, A. K. & Balasubramanian, K. K. Microwave-induced, Montmorillonite K10-catalyzed Ferrier rearrangement of tri-O-acetyl-D-galactal: mild, eco-friendly, rapid glycosidation with allylic rearrangement. *Tetrahedron Lett.* **43**, 6795–6798 (2002).
  15. Rokade, S. M. & Bhate, P. M. Ferrier reaction in a deep eutectic solvent. *Carbohydr. Res.* **415**, 28–30 (2015).
  16. Yan, M., Kawamata, Y. & Baran, P. S. Synthetic Organic Electrochemical Methods Since 2000: On the Verge of a Renaissance. *Chem. Rev.* **117**, 13230–13319 (2017).
  17. Frontana-Urbe, B. A., Little, R. D., Ibanez, J. G., Palma, A. & Vasquez-Medrano, R. Organic electrosynthesis: a promising green methodology in organic chemistry. *Green. Chem.* **12**, 2099–2119 (2010).
  18. Badsara, S. S., Ucheniya, K., Chouhan, A. & Gurjar, A. Electrochemical Synthesis: An Alliance of Electrochemistry and Organic Synthesis for Value-Added Moieties. *The Chemical Record* e202500092 (2025).
  19. Qi, C., Goti, G., Sartorel, A., Dell'Amico, L. & Mazzarella, D. Electrochemical Ferrier Rearrangement of Glycals. *Org. Lett.* **26**, 9328–9333 (2024).
  20. Noël, T., Cao, Y. & Laudadio, G. The Fundamentals Behind the Use of Flow Reactors in Electrochemistry. *Acc. Chem. Res.* **52**, 2858–2869 (2019).
  21. Regnier, M., Vega, C., Ioannou, D. I. & Noël, T. Enhancing electrochemical reactions in organic synthesis: the impact of flow chemistry. *Chem. Soc. Rev.* **53**, 10741–10760 (2024).
  22. Capaldo, L., Wen, Z. & Noël, T. A field guide to flow chemistry for synthetic organic chemists. *Chem. Sci.* **14**, 4230–4247 (2023).
  23. Takumi, M., Sakaue, H. & Nagaki, A. Flash Electrochemical Approach to Carbocations. *Angew. Chem. Int Ed.* **61**, e202116177 (2022).
  24. Yoshida, J., Shimizu, A. & Hayashi, R. Electrogenenerated Cationic Reactive Intermediates: The Pool Method and Further Advances. *Chem. Rev.* **118**, 4702–4730 (2018).
  25. Sato, E. et al. Electrochemical carbon-ferrier rearrangement using a microflow reactor and machine learning-assisted exploration of suitable conditions. *Org. Process Res. Dev.* **28**, 1422–1429 (2024).
  26. Heard, D. M. & Lennox, A. J. J. Electrode materials in modern organic electrochemistry. *Angew. Chem. Int Ed.* **59**, 18866–18884 (2020).
  27. Kooli, A. et al. Electrochemical hydroxylation of electron-rich arenes in continuous flow. *Eur. J. Org. Chem.* **2022**, e202200011 (2022).
  28. Ošeka, M. et al. Electrochemical aziridination of internal alkenes with primary amines. *Chem* **7**, 255–266 (2021).
  29. Laktsevich-Iskryk, M. et al. Telescoped synthesis of vicinal diamines via ring-opening of electrochemically generated aziridines in flow. *J. Flow. Chem.* **14**, 139–147 (2024).
  30. Laudadio, G., de Smet, W., Struik, L., Cao, Y. & Noël, T. Design and application of a modular and scalable electrochemical flow microreactor. *J. Flow. Chem.* **8**, 157–165 (2018).
  31. Hunt, K. E. et al. Interplay of monosaccharide configurations on the deacetylation with *Candida antarctica* lipase-B. *J. Org. Chem.* **90**, 663–671 (2025).
  32. Kawabata, H., Kubo, S. & Hayashi, M. Reaction of D-glycals with azidotrimethylsilane. *Carbohydr. Res.* **333**, 153–158 (2001).
  33. Heyns, K. & Hohlweg, R. [3.3]-Sigmatrope Umlagerungen an Glycalen und Pseudoglycalen. *Chem. Ber.* **111**, 1632–1645 (1978).
  34. Carlson, A. S. & Topczewski, J. J. Allylic azides: synthesis, reactivity, and the Winstein rearrangement. *Org. Biomol. Chem.* **17**, 4406–4429 (2019).
  35. McElroy, C. R., Constantinou, A., Jones, L. C., Summerton, L. & Clark, J. H. Towards a holistic approach to metrics for the 21st century pharmaceutical industry. *Green. Chem.* **17**, 3111–3121 (2015).
  36. Morlacci, V. et al. Electrocatalytic hydrogen evolution reaction enabling cyanation of electron-poor carbons with acetone cyanohydrin. *Eur. J. Org. Chem.* **27**, e202400236 (2024).
  37. Köckinger, M. et al. Sustainable electrochemical decarboxylative acetoxylation of aminoacids in batch and continuous flow. *Green. Chem.* **23**, 2382–2390 (2021).

## Acknowledgements

This work was supported by the Ministry of Education and Research of Estonia through the Centre of Excellence in Circular Economy for Strategic Mineral and Carbon Resources (SOURCES, TK228, 01.01.2024–31.12.2030) and by the Estonian Research Council grants (PSG828, PRG1031 and Estonian sub-project ETAG24073 of NordForsk project AGRI-WASTE2H2). The authors would also like to thank Tatsiana Jarg for the HRMS analysis and Nora Deil for the assistance with disaccharide synthesis.

## Author contributions

P.S. and M.F. have performed the experiments. K.E.H. has contributed to disaccharide synthesis. T.K. has contributed to the work supervision. D.M. has conceived the idea and supervised the work. M.O. has designed the experiments, supervised the work and secured the fundings. P.S. has written the manuscript with contributions from all authors.

## Competing interests

The authors declare no competing interests.

## Additional information

**Supplementary information** The online version contains supplementary material available at <https://doi.org/10.1038/s42004-026-01948-1>.

**Correspondence** and requests for materials should be addressed to Daniele Mazzarella or Maksim Ošeka.

**Peer review information** *Communications Chemistry* thanks the anonymous reviewers for their contribution to the peer review of this work.

**Reprints and permissions information** is available at <http://www.nature.com/reprints>

**Publisher's note** Springer Nature remains neutral with regard to jurisdictional claims in published maps and institutional affiliations.

**Open Access** This article is licensed under a Creative Commons Attribution-NonCommercial-NoDerivatives 4.0 International License, which permits any non-commercial use, sharing, distribution and reproduction in any medium or format, as long as you give appropriate credit to the original author(s) and the source, provide a link to the Creative Commons licence, and indicate if you modified the licensed material. You do not have permission under this licence to share adapted material derived from this article or parts of it. The images or other third party material in this article are included in the article's Creative Commons licence, unless indicated otherwise in a credit line to the material. If material is not included in the article's Creative Commons licence and your intended use is not permitted by statutory regulation or exceeds the permitted use, you will need to obtain permission directly from the copyright holder. To view a copy of this licence, visit <http://creativecommons.org/licenses/by-nc-nd/4.0/>.

© The Author(s) 2026